geologicaacta

Petrogenesis of highly fractionated I-type peraluminous granites: La Pedriza pluton (Spanish Central System)

CECILIA PÉREZ-SOBA [1] and CARLOS VILLASECA [1]

[1] Department of Petrology and Geochemistry, Universidad Complutense de Madrid- Instituto de Geología Económica (C.S.I.C.)
c/ José Antonio Novais, 2, 28040 Madrid, Spain. Pérez-Soba E.mail: pesoa@geo.ucm.es

─┤ A B S T R A C T ├─

The La Pedriza pluton stands out as the most extensively fractionated granite (Rb < 629; Sr < 2 and Ba < 2 ppm) of the Spanish Central System Batholith. These granites show a strong enrichment in some rare metal contents (Nb = 44, Y = 136, Yb = 10.7, U = 17, Ta = 7, Sc = 15 ppm). The petrography and geochemistry (including Sr-Nd isotopes) reveal that the pluton is composed of at least four units. These are classified as I-type peraluminous leucogranites (A/CNK=1.03-1.17), P-poor (P_2O_5<0.2 wt%) and Na_2O-rich (< 4.24 wt%) exhibiting differences in their HFSE and REE contents and εNd compositions. Moreover, the units of the La Pedriza granite display different trends of fractional crystallization. REE spectra of the two most fractionated units suggest the involvement of a fluorine-rich melt in the last stages favouring the crystallization of xenotime and niobotantalates. Intermediate meta-igneous granulite protoliths are proposed as source rocks. The most evolved units of the La Pedriza pluton show chemical features convergent to A-type granites; these are explained by extensive fractional crystallization of a P-poor, I-type granite magma.

KEYWORDS | Hercynian-Variscan orogeny. Peraluminous I-type granites. High field strength elements. Multiple intrusions.

INTRODUCTION

Peraluminous high-silica magmatic rocks rich in high-field strength elements (HFSE) and rare earth elements (REE) have been the focus of numerous studies for decades (c.f. Mackenzie et al. 1988; c.f. Champion and Chappell, 1992). The chemical and mineralogical characteristics of these rocks (plutonic or volcanic) have been considered to reflect different source rocks and/or protracted magmatic histories, mainly fractional crystallization (e.g. Christiansen et al. 1986; Kostitsyn et al., 2007). Nevertheless, some authors have suggested the involvement of a fluid residual or hydrothermal phase (c.f. Mackenzie et al., 1988). Their extremely felsic composition (SiO_2>72%) close to minimum-temperature melts acquired after a long fractionation history makes discerning their magma sources and melting conditions difficult. Highly fractionated granites (varieties rich in rare metals) overlap in different mineral, geochemical and petrogenetic classifications (Loiselle and Wones, 1979; Chappell and White, 1992; King

et al., 1997, 2001; Whalen et al., 1987; Landenberger and Collins, 1996). Discussion still continues (Martin, 2007) even where restricted to low-P granites (i.e. excluding F-Li-rich S-type granites) as evolved REE-HFSE-rich granites may be either classified as highly fractionated I-type (e.g. Whalen, 1983; Champion & Chappell, 1992) or A-type granites (e.g. King et al., 2001).

La Pedriza is a highly fractionated granite pluton in the Hercynian Spanish Central System (SCS) showing one of the highest rare-metal contents among the Iberian Hercynian granites. This enrichment is correlated with a marked depletion in compatible elements in granite liquids (e.g. Sr, Ba, Eu). Highly fractionated I-type granites have been rarely described in the Iberian Hercynian Belt. In previous studies (Pérez-Soba, 1992; Pérez-Soba et al., 2001), three main intrusive units were established in the La Pedriza pluton based in mineral and whole-rock compositions. The aim of the present study is to discuss the petrogenesis and evolution of the pluton using new whole-rock analytical data (major and trace elements, and Sr-Nd isotopes). The geochemical characteristics of the constituent granite units do not define a single suite, suggesting a complex history of closely related peraluminous granite pulses.

GEOLOGICAL SETTING

The SCS is the innermost continental region of the Iberian Belt. In this axial part, the crustal thickening is estimated to have reached at least 70-80 km, triggering in their mid-to-lower levels a widespread granulitic metamorphic regime (Barbero and Villaseca, 2000). The Hercynian metamorphism evolved from high-P eclogite facies towards low-P high-T granulite facies conditions (Barbero and Villaseca, 2000); the metamorphic peak was reached at ca 335 Ma in a tectonic scenario of extensional collapse (Doblas et al., 1994; Escuder Viruete et al., 1998; Bea et al., 2003; Montero et al., 2004; Castiñeiras et al., 2008).

The SCS batholith started its formation ca 10 Ma after the metamorphic climax as the main period of plutonic intrusion occurred, in a post tectonic context, from 324-285 Ma (Villaseca et al., 1995; Bea et al., 1999). The granitoids, mainly felsic and peraluminous in composition, have been divided into three subgroups (Villaseca et al., 1998): i) strongly peraluminous cordierite-bearing granites of S-type affinity with Al-rich biotite and monazite as characteristic phases, ii) metaluminous-peraluminous I-type granites with Al-poor biotite, amphibole and allanite and iii) slightly peraluminous biotite granites showing characteristics transitional between the other two subgroups. As these granites show similar initial isotopic ratios, Villaseca et al. (1998) consider that all derived from

similar meta-igneous sources. These I- and S-type granite plutons outcrop along the SCS batholith axis, with no pattern to their spatial or temporal distribution (Villaseca et al., 1998; Bea et al., 2003) (Fig.1a). The La Pedriza pluton rock has been classified as peraluminous I-type granite (Villaseca et al., 1998).

The La Pedriza pluton outcrops over some 75 km^2 with an exposed height of 1000 m in the eastern part of the SCS. The pluton is divided into western and eastern sectors, locally in contact over less than one kilometre (Fig. 1b). The E margin mainly consists of an aplo-pegmatitic body which approaches nearly 200 m in width. In other marginal sectors discontinuous aplo-pegmatitic rocks appear and, on the NE margin, some pegmatites pods may include magnetite, beryl or garnet. A set of branched synplutonic aplitic veins, cutting the contact with monzogranite wall-rock, disappear 200 m beyond the contact.

The pluton is intrusive into metamorphic- and other post-tectonic peraluminous granite rocks (Fig.1a). Field relations indicate that its level of emplacement was epizonal. Thermal metamorphism is observed within intruded granites on the eastern pluton wall (Fig 2) where a 100 m wide aureole is developed with sillimanite and andalusite aggregates with albite-rich plagioclase. Moreover, in the aplitic-pegmatitic facies of the eastern margin, Sánchez-Muñoz et al. (1990) determined a low solidus temperature of crystallization of < 500ºC in a volatile-rich environment (F, CO$_2$).

A whole-rock Rb-Sr isochron of 307 ± 3 Ma (MSWD = 1.41) for the La Pedriza leucogranites has been established (Pérez-Soba, 1992). More recently, SHRIMP U-Pb ages in primary and metamictic zircon crystals of the more evolved unit have yielded a 324-300 Ma age range (Nasdala et al., 2009).

ANALYTICAL PROCEDURES

17 new samples of the La Pedriza leucogranites were analyzed for whole-rock major- and trace elements at Activation Laboratories (Canada). The samples were fused using LiBO$_2$ and dissolved with HNO$_3$. Solutions were analysed by inductively coupled plasma atomic emission spectrometry (ICP-AES) for major elements and trace elements were determined by ICP mass spectrometry (ICP-MS). Uncertainties in major elements are generally between ±1 and ±3% whereas most of the trace elements have uncertainties < ±10 %. REE precision and accuracy have been estimated using two international standards (Table A1, electronic appendix). Mass interferences on REE contents have been corrected (Table A2, electronic appendix), thus the lanthanide tetrad effect in some of the studied samples are not analytical artifacts. In selected samples, F and Li
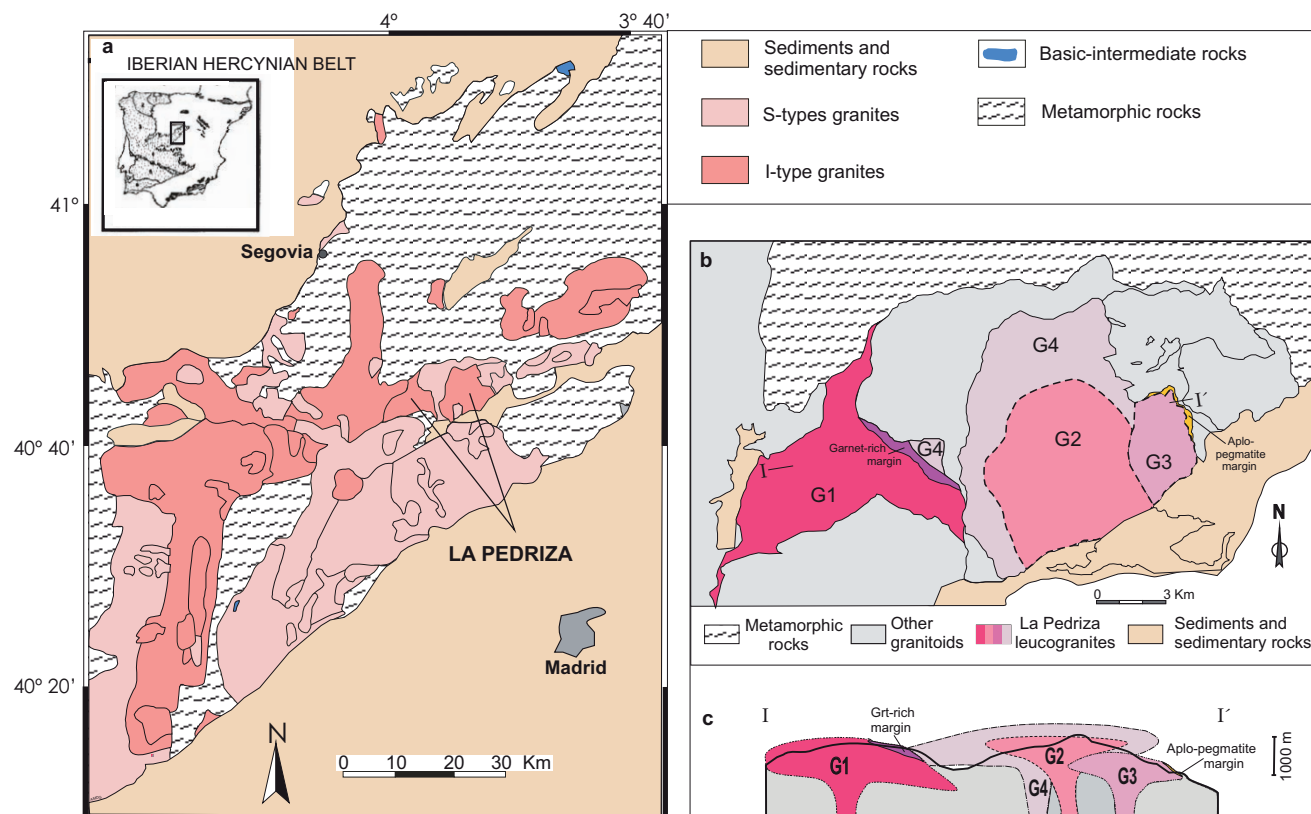
FIGURE 1 | a) Generalized geological map of the eastern part of the Spanish Central System (Sierra de Guadarrama sector), showing the distribution of S- and I-type granite plutons and the localization of the two bodies (eastern and western) of the La Pedriza Pluton. b) Distribution of the four granite units comprising the La Pedriza pluton. c) A W-E cross-section showing the emplacement of magma pulses into the metamorphic- and older granitic host rocks. The more fractionated G4 unit could be the first granite pulse as is usually the case in high silica plutons where more fractionated and volatile-rich magmas accumulate towards the top.

contents were determined in the laboratory of the Spanish Geologic and Mining Institute (IGME). F was extracted by pyrohydrolysis and the element abundance was determined by spectrophotometric methods. After sample digestion with HF-HNO$_3$-HClO$_4$, Li was determined by atomic absorption spectrophotometry. An analytical error of ±10% is estimated based on the analysis of a certificated standard. Representative analyses of the four units of the La Pedriza pluton, including 4 analyses from Pérez-Soba (1992), are presented on Table 1.

Six samples were selected for Sr-Nd isotopic analyses at the *CAI de Geocronología y Geoquímica Isotópica* of the Complutense University of Madrid using an automated VG Sector 54 multicollector thermal ionisation mass spectrometer with data acquired in multidynamic mode. The Sr-Nd analytical procedures used in this laboratory have been described by Reyes et al. (1997). Repeated analysis of NBS 987 gave $^{87}Sr/^{86}Sr = 0.710249 \pm 30$ (2σ, n=15) and $^{143}Nd/^{144}Nd = 0.511809 \pm 20$ (2σ, n=13) for the JM Nd standard. The 2σ error for calculated εNd values is ± 0.4. εNd$_{(t)}$ was calculated relative to Chondrite Uniform Reservoir (CHUR) present-day values, i.e.

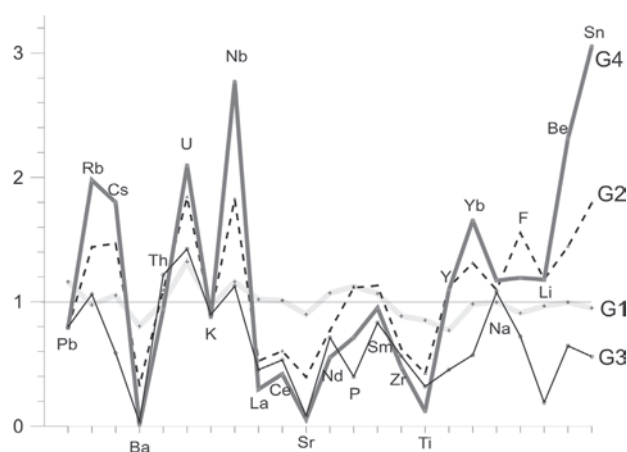$^{147}Sm/^{144}Nd = 0.1967$, $^{143}Nd/^{144}Nd = 0.512638$ (Jacobsen and Wasserburg, 1980).

FIGURE 2 | Enrichment-factor diagram of the four units of the La Pedriza pluton. Data for G1 to G4 are based on the average compositions of all samples from each pulse. These averages are normalized to sample 87225 (G1 pulse) as parental melt composition.

TABLE 1 | **Major (in wt. %) and trace element (in ppm) data of La Pedriza leucogranites.**

Type	G1	G1	G1(*)	G1	G2	G2(*)	G2	G2	G3(*)	G3	G3	G4(*)	G4	G4	G4	G4
Sample	68931	87225	87868	107032	106042	87161	106043	106041	66622	106044	107031	87059	106045	105575	105562	107026
SiO_2	72.73	74.21	74.56	76.14	74.78	75.24	75.91	76.6	76.44	77.44	77.5	75.12	76.52	76.56	76.98	76.81
TiO_2	0.13	0.15	0.11	0.12	0.07	0.06	0.06	0.07	0.04	0.05	0.04	0.01	0.01	0.02	0.01	0.01
Al_2O_3	13.99	13.19	13.11	12.79	13.43	13.03	13.12	13.04	12.1	12.67	12.34	12.85	12.88	13.08	13.09	13.08
Fe_2O_3t	1.69	1.72	1.83	1.65	1.09	1.22	1.02	1.14	1.08	0.97	1.1	0.85	0.83	0.93	0.91	0.94
MnO	0.04	0.04	0.04	0.04	0.03	0.03	0.03	0.03	0.02	0.02	0.02	0.03	0.04	0.03	0.05	0.07
MgO	0.19	0.19	0.17	0.16	0.11	0.08	0.1	0.15	0.02	0.03	0.02	0.01	0.02	0.01	0.04	0.02
CaO	0.93	1.05	0.86	0.78	0.36	0.6	0.49	0.31	0.51	0.4	0.49	0.43	0.32	0.22	0.19	0.26
Na_2O	3.67	3.47	3.47	3.39	3.72	3.9	3.91	3.69	3.7	3.7	3.86	4.24	4.12	4.03	3.99	4.17
K_2O	5.07	4.65	4.85	4.55	4.71	4.51	4.22	4.46	4.5	4.35	4.33	4.28	4.13	4.36	4.3	4.14
P_2O_5	0.07	0.05	0.16	0.04	0.04	0.11	0.06	0.05	0.11	0.03	0.01	0.08	0.02	0.02	0.02	0.02
LOI	0.68	0.58	0.65	0.43	0.77	0.63	0.81	0.65	0.32	0.58	0.31	0.83	0.55	0.59	0.63	0.43
Total	99.2	99.3	99.41	99.93	98.99	99.3	99.63	100.07	98.74	100.14	99.92	98.65	99.36	99.76	100.12	99.85
A/CNK	1.07	1.05	1.06	1.08	1.14	1.06	1.11	1.14	1.03	1.1	1.04	1.05	1.09	1.12	1.13	1.11
F	602	865	753	n.d.	355	1540	2371	446	745	36	n.d.	2146	2444	116	1176	n.d.
Li	55	62	n.d.	n.d.	91	121	141	51	n.d.	40	n.d.	n.d.	287	36	246	n.d.
Rb	257	239	254	223	365	327	443	351	269	266	255	516	629	471	628	493
Cs	9	7.2	n.d.	6.7	12.4	n.d.	12.1	7.9	n.d.	4.1	4.1	n.d.	21.5	5.6	15	10.8
Sr	43	45	35	33	23	23	24	22	3	4	2	1	1	5	2	1
Ba	298	334	217	253	97	100	100	110	10	11	3	1	2	17	5	3
Ga	19	15	15	17	23	25	23	22	9	19	19	24	26	25	26	25
Nb	12	12	14	11.6	22	24	28	23	13	17	14	44	33	37	36	25
Zr	137	119	96	125	83	79	65	93	68	54	73	66	55	74	59	41
Th	32.6	21.9	23	21.8	25.1	26	22.6	26.3	21	36	32.6	27	21.2	21.4	19.5	18.3
U	7.7	5.3	n.d.	5.9	7.6	n.d.	16.9	7.2	n.d.	6.9	8.8	n.d.	14.3	8.8	10.5	11.1
Sn	7	7	n.d.	6	11	n.d.	15	12	n.d.	5	4	n.d.	22	28	21	17
Y	67	49	50	44	69	70	74	55	28	14	44	136	53	104	36	83.1
La	40.5	29.7	28.34	22.2	13.36	16.84	13.07	14.23	18.86	11.04	13.9	12.55	5.22	6.62	4.93	12.5
Ce	86.6	62.9	58.11	60	33.29	45.71	32.71	35.34	43.72	25.37	35.7	46.01	18.66	22.12	12.15	35
Pr	10.1	7.31	n.d.	5.84	4.36	n.d.	4.36	4.42	n.d.	3.45	4.75	n.d.	2.02	2.55	1.56	4.63
Nd	37.8	27	26.14	23.6	20.45	21.32	21.03	20.27	22.19	14.41	22.9	22.58	10.24	12.63	7.07	24.1
Sm	9.76	6.98	7.37	6	7.93	8.45	8.34	7	6.81	3.99	6.78	12.52	5.1	6.86	2.74	8.81
Eu	0.46	0.44	0.44	0.31	0.12	0.2	0.13	0.14	0.11	0.03	0.02	0.1	0	0.02	0.01	0.01
Gd	10.1	7.28	6.77	6.09	9.99	8.72	10.26	8.16	6.2	3.64	7.47	14.83	7.22	10.73	3.78	10.9
Tb	1.9	1.4	n.d.	1.15	2.25	n.d.	2.3	1.81	n.d.	0.62	1.34	n.d.	1.75	2.87	1.05	2.28
Dy	11.4	8.48	7.65	7.57	13.18	10.78	13.43	10.59	5.52	3.35	7.94	19.25	11.14	17.41	7.16	15.1
Ho	2.26	1.71	n.d.	1.5	2.47	n.d.	2.55	1.95	n.d.	0.63	1.59	n.d.	2.16	3.29	1.5	2.93
Er	7.23	5.25	4.23	4.82	8.25	5.84	8.35	6.56	2.85	1.98	4.81	10.19	7.25	11.09	5.54	9.42
Tm	1.1	0.81	n.d.	0.73	1.32	n.d.	1.31	1.03	n.d.	0.29	0.71	n.d.	1.26	1.79	0.99	1.52
Yb	6.85	5.1	4.35	4.71	7.48	5.93	7.47	6.04	3.01	1.71	4.19	10.61	8.46	10.48	6.25	9.65
Lu	1	0.74	0.68	0.69	1.08	0.96	1.08	0.87	0.52	0.25	0.59	1.58	1.22	1.52	0.94	1.39
K/Rb	164	162	159	169	107	115	79	105	139	140	141	69	55	77	57	70
TE_3	1.07	1.08	n.d.	1.08	1.21	n.d.	1.2	1.21	n.d.	1.05	1.04	n.d.	1.23	1.31	1.27	1.15
$TE_{1,3}$	1.06	1.06	n.d.	1.1	1.1	n.d.	1.09	1.11	n.d.	1.03	1.02	n.d.	1.19	1.22	1.13	1.07

Fe_2O_3t is total Fe as Fe_2O_3. n.d. = not determined. (*) Analyses from Pérez-Soba (1992)

$Ce^* = Ce_N/La_N^{2/3} xNd^{1/3})$, $Pr^*=Pr_N/(La_N^{1/3} xNd_N^{2/3})$, $Tb^*=Tb_N/(Gd_N^{2/3} xHo_N^{1/3})$, $Dy^*=Dy_N/(Gd_N^{1/3} xHo_N^{2/3})$, $TE_3=(Tb^* xDy^*)^{1/2}$, $TE_{1,3}=(TE_1 xTE_3)^{1/2}$, $TE_1=(Ce^* xPr^*)$

PETROGRAPHY AND MINERALOGY

The La Pedriza pluton is a coarse- to medium-grained leucogranite, variably pink-coloured mainly in the eastern sector. The leucogranite looks texturally very homogeneous although, towards the contact, the grain size may diminish. Based on mineralogical and geochemical criteria, the La Pedriza pluton has been divided into four units (G1 to G4) which show an irregular distribution (Fig. 1b). The G1 unit mainly constitutes the western granitic massif and represents the less evolved pulse developing, at the northeastern margin of the massif, a garnet-bearing cupola. The G2 and G4 granites are the main units in the eastern body of the pluton (Fig. 1b) whereas the G3 unit is limited to the southeastern margin. The small portion of the G4 unit cropping out in the NE margin of the western body shows some compositional differences when compared with the main G4 outcrops. The

presence of an aplo-pegmatite granite cupola at the margin of the G3 unit suggests an upper intrusive contact at least 1000 m below the G2 and G4 units (Fig. 1c). Although the La Pedriza pluton shows considerable height differences between units (from 2000 to 950m), no correlated compositional changes were noted.

The granite contains few enclaves. The enclaves are i) xenolithic plutonic wall-rocks, ii) acid microgranular enclaves and iii) milky quartz globules and surmicaceous enclaves. The last are probably mostly digested me–tamorphic xenoliths.

The La Pedriza leucogranites consist of mi–crophertitic K-feldspar, quartz, plagioclase (An_{32-1}) and accessory biotite (Table 2). Zircon, apatite, xenotime and monazite are the common accessory minerals; other accessories occur only in some units (Table 2;

TABLE 2 | **Petrographic features of significant phases in the units from La Pedriza pluton.**

	G1		G2	G3	G4
	main zone	garnet bearing margin			
Plagioclase	subhedral, cumulophyric, weakly zoned, myrmekite $Ab_{80(67-98)}$	subhedral, cumulophyric weakly zoned, myrmekite $Ab_{96(94-99)}$	subhedral, myrmekite $Ab_{92(90-93)}$	euhedral-subhedral, myrmekite $Ab_{92(85-98)}$	subhedral, myrmekite $Ab_{96(95-99)}$
Alkali-feldspar	anhedral microcline perthitic	anhedral microcline perthitic	anhedral microcline perthitic	subhedral microcline perthitic	anhedral microcline perthitic
Trioctahedral micas	sub - euhedral early	sub - euhedral early	sub- anhedral late	sub- anhedral late	sub- anhedral late
abundance	3-4 %	3%	2%	2%	2%
Fe^{2+}_{total}	3.69 *(3.52-3.89)*	3.23 *(3.14-3.37)*	3.16 *(3.06-3.27)*	4.09 *(3.92-4.54)*	2.53 *(2.26-2.94)*
Ti	0.31 *(0.30-0.35)*	0.08 *(0.06-0.11)*	0.18 *(0.15-021)*	0.24 *(0.10-0.34)*	0.04 *(0.02-0.07)*
Al^{vi}	0.58 *(0.55-0.64)*	1.13 *(1.10-1.15)*	1.63 *(1.44-1.95)*	0.83 *(0.71-1.09)*	1.73 *(1.59-1.93)*
Mn	0.10 *(0.09-0.12)*	0.17 *(0.13-0.21)*	0.10 *(0.08-0.11)*	0.12 *(0.10-0.14)*	0.21 *(0.14-0.32)*
Accessory minerals	Zrn, F-Ap, Ilm, Mnz, Aln, Xtm, Fl, Urn, Tho	Zrn, F-Ap, Ilm, Mnz, Xtm, Fl, Tho, Grt, Rt	Zrn, F-Ap, Ilm, Fl, Mnz, Xtm, Mn-col, U-py, Nb-Rt, Tho	Zrn, Mnz, F-Ap, Mt, Fl, Aln, Xtm, U-Tho	Xtm, Zr, F-Ap, Mnz

Mineral abbreviations according to Kretz (1983). Other minerals: F-Ap = fluor-apatite, Mn-col = mangano-columbite, Nb-Rt = Nb-rich rutile, Tho = thorite, Urn = uraninite, U-py= Urano-pyrochlore, U-tho = urano-thorite, Xtm = xenotime. Biotite: averaged values in cationic abundances based on 22 oxygens (in brackets, compositional ranges).

Casillas et al., 1995; González del Tánago et al., 2004). Accessories are mainly hosted in trioctahedral micas but also in feldspars and quartz. The presence and proportions of accessory minerals, and the colour of biotite, are the main basis for the petrographical subdivision of the La Pedriza pluton. The main petrographical and mineral compositional features of the La Pedriza leucogranites are summarized below.

K-feldspar crystallized after quartz and plagioclase, and generally with biotite. It is characterized by an increase in the microcline variety from G2 to G3 to G4. K-feldspar from G1 and G3 is less rich in the albite-component (Ab_{3-9} in G1 and Ab_{7-1} in G3) when compared to the other units (Ab_{1-13} in G2, Ab_{2-12} in G4).

Plagioclase occurs as poorly-zoned, subhedral to anhedral crystals. The average compositions are $An_{18\ (36-1)}$ in G1, $An_{7\ (8-6)}$ in G2, $An_{7,\ 12-1)}$ in G3 and $An_{3\ (4-1)}$ in G4. An intergranular albite-rich plagioclase film (in some cases, myrmekitic) is commonly developed between plagioclase and K-feldspar crystals.

Biotite is the main mafic mineral in the La Pedriza leucogranites. It occurs as subhedral to euhedral flakes, reddish in colour in G1, pleochroic greenish-brown to bluish-green in G3, and pleochroic light-green to colourless in the G2 and G4 units. They are mostly true

trioctahedral micas except for the light-green varieties in G2 and G4 (2.43 < M site < 2.49 atoms per formula unit). The biotite has been classified using the diagram of Tischendorf et al. (2001), with Li_2O contents estimated using the empirical formula proposed by Tischendorf et al. (1997). The mica is annite to Fe-rich siderophillite in G1 and G3, siderophyllite in G2, and siderophyllite close to protolithionite in composition in the garnet-bearing zone of G1 and G4 where it overgrows earlier siderophyllite. Biotite from the G1 garnet-bearing zone is richer in Mn and poorer in Mg compared to micas from the rest of the unit.

Ilmenite is the main oxide in the pluton. Its Mn content is one of the highest in the SCS granites (Villaseca and Barbero, 1994). Primary magnetite (as zoned euhedral to subeuhedral crystal associated with biotite), occurring in the G3 unit and in some samples of the G4 unit, shows exsolved hematite both in the leucogranite and in pegmatites. The La Pedriza pluton is the only referenced pluton in the SCS with magnetite. Zoned euhedral rutile is occasionally found in the garnet-rich margin of G1 and in G4 (González del Tánago et al., 2004).

Zircon occurs as large oscillatory euhedral crystals in the G1 and G3 units, although significantly more equant and smaller in G3. Hf-rich zircon appears in the garnet-bearing G1 zone (< 13.60 wt% of Hf_2O). In G2 and G4,

the dominant zircon is an alveolar type (Pérez-Soba et al., 2007), commonly occurring in association with xenotime and thorite, and occasionally with monazite and apatite. This latter type is richer in Y, HREE, U, Th and divalent cations, particularly so in the G4 unit where maximum contents (in wt%) of $Y_2O_3 < 10.23$; $ThO_2 < 4.75$, $UO_2 < 4.83$ and $HRRE_2O_3 < 5.69$ are reached. Zoned crystals show decreasing Zr and increasing Y, HREE, U and Th towards their rims (Pérez-Soba et al., 2007).

Fluorapatite (< 3.3 wt% F) is present in all four units. It is abundant in G1 as acicular euhedral crystals included in plagioclase and biotite. It is less abundant in G2 and G4 where it occurs as larger euhedral crystals included in biotite. Fluorapatite is rare in G3 and, when present, is associated with other interstitial accessory minerals included in fluorite.

Monazite occurs in all units although markedly less abundant in G4. It appears either as oscillatory-zoned subhedral- or anhedral (alveolar) crystals. Monazite usually occurs as independent grains, but in the G2 and G4, may be associated mainly with xenotime. The monazite is rich in Th; similar ThO_2 averages (ca 5-7 wt%) characterize the mineral in the four units although higher contents (< 18 wt%) are found in G2. Monazite chondrite-normalized REE spectra (not shown) are similar in all granite units.

Y-Xenotime is present in all the leucogranites, being dominant in G4. It occurs as euhedral oscillatory-zoned crystals included in biotite and feldspars. Crystals are richer in HREE and Y towards their rims, and commonly associated to zircon and monazite. Xenotime also occurs as anhedral alveolar crystals. Contents of UO_2 (< 4.3 wt%) and ThO_2 (< 8.35 wt%) are higher in xenotime from G2. Chondrite-normalized REE spectra are similar for the four units, with well defined first and third tetrad effects, and showing a negative Pr anomaly in the LREE pattern (not shown).

Allanite and thorite occur in the G1, G2 and G3 units. Allanite occurring as euhedral zoned crystals displaying a high degree of metamictization is very common in G3. Thorite occurs as anhedral crystals in the G2 and G3 units and as drop-like inclusions with xenotime in G1. The thorite has similar chondrite-normalized REE spectra and compositions in all three units.

Garnet is exclusively found in the northeastern cupola of the G1 unit (Fig. 1b). It occurs as zoned, anhedral magmatic crystals of $Alm_{48-75}Sp_{49-24}Gros_{5-0}Pyr_{0-2}$ composition. Spes–sartine and grossular increase, and almandine and pyrope decrease rimwards (profile III in Fig. 6 of Villaseca and Barbero, 1994).

Fluorite, irregularly distributed within the pluton, is more common in G3 and G2. In G2 unit is found as small xenomorphic crystals interleaved in plagioclase whereas, in G3, it occurs interstitially within accessory-rich clusters.

G4 occasionally contains late-magmatic muscovite, beryl in one small miarolitic cavity on the NE margin of the unit, Y-columbite, Mn-columbite and U-pyrochlore (this last also in G3). Uraninite has been reported only from G1 (Brandebourger, 1984).

Each unit of the La Pedriza pluton shows a slightly different pattern of secondary alteration. In G1 and G3, secondary muscovite and chlorite is less common than in G4. In G2, biotite exhibits a marked alteration to chamosite. In the most evolved units (G2 and G4), Ce-bastnaesita and Y-aeschynite are probably products of late to postmagmatic remobilization (González del Tánago et al. 2004).

GEOCHEMISTRY

Major and trace elements

The La Pedriza leucogranites show high contents (in wt%) of SiO_2 (72.7-77.5), K_2O (4.0-5.3), and low contents of CaO (0.2-1.1), MgO (0.01-0.25), Fe_2O_3t (0.8-1.9) and TiO_2 (< 0.17) (Table 2). When compared to other SCS granites (Villaseca et al., 1998; Bea et al., 1999), they reach the highest contents of Na_2O (3.2-4.2 wt%) and the lowest of P_2O_5 (< 0.2 wt%). All of the analyzed samples show high contents of alkalies (> 8 wt%) with a marked decrease in K_2O from G1 to G4. All samples are peraluminous in composition (A/CNK [molecular $Al_2O_3/CaO+Na_2O+K_2O$] = 1.03-1.17), without significant variation between units (Table 2), and they are subalkaline (K_2O+Na_2O = 7.9-8.9 wt%), with a peralkalinity index ranging from 0.47-0.56. On an Ab-An-Q normative diagram, the leucogranites plot near to minimum temperature melts, although some Ab enrichment in the G4 unit is apparent.

The La Pedriza leucogranites are characterized by high contents (in ppm) of the alkali metals Rb (< 629), Cs (< 22) and Li (< 287); and of some HFSE, namely, Y (< 136), Nb (< 44), Sn (< 28), Ta (< 7), Th (< 36), U (< 17), Sc (4-15), and Pb (20-65). They have very low contents of Ba (1-369), Sr (1-56), Eu (< 0.5), Zr (37-137) and Hf (3-6) and a wide range of REE (56-227) (Table 1). Normalized to the least evolved sample of the pluton (Fig. 2), the G4 unit is the most enriched in Rb, Cs, U, Nb, Yb, Be and Sn, slightly low in La, Ce, Nd, P and Zr and extremely impoverished in Ba, Sr, Eu and Ti contents.
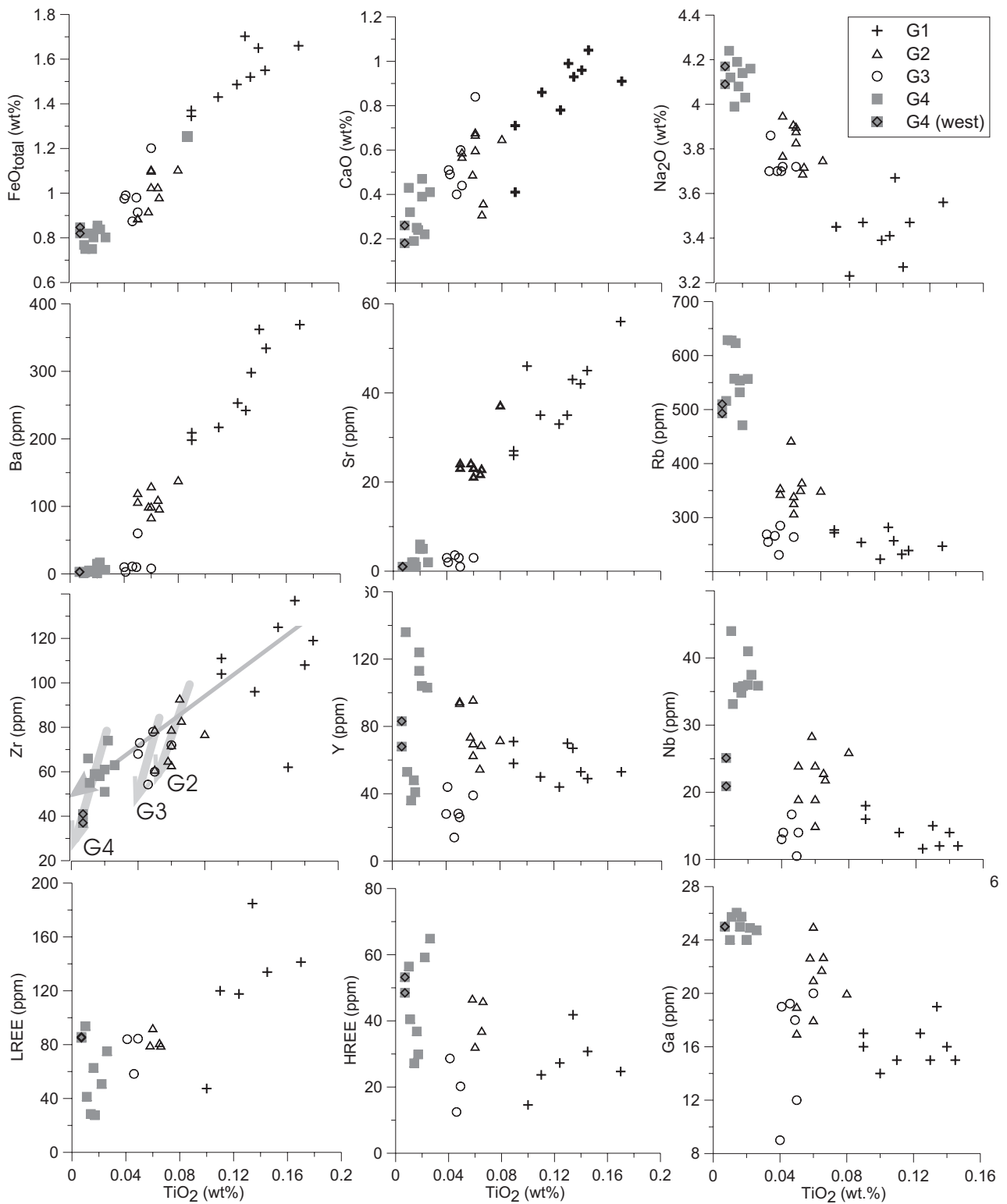
FIGURE 3 | Variation diagrams of TiO$_2$ vs. selected major- and trace elements for the units of the La Pedriza leucogranites. In the TiO$_2$ vs. Zr plot, both general and individual unit evolution lines are indicated.

Using TiO_2 as a differentiation index, the most striking features are compositional gaps and slope changes between unit trends (Fig. 3). Thus, CaO FeOt, MgO, K_2O, Sr, Ba, Zr, Eu and LREE behave as compatible components, decreasing from G1 to G4, but with different trends. The G1 granites follow an extended line of evolution contrasting with the limited variation shown by the other units. Extremely low contents of Sr (~1 ppm), Ba (~1 ppm) and Eu/*Eu (~0.01) characterize the G3 and G4 units (Fig. 3). The G2 and G4 units are, on the other hand, relatively enriched in Na_2O, Rb, Nb, Y, HREE, Cs, Ga, Sn, F, Li, Mn, Ta and Hf. The two westernmost samples from G4 plot apart from the main G4 group, e.g. Zr and Nb in Figure 3. Other components such as Al_2O_3, P_2O_5, U, Th and Pb do not show clear trends, although higher contents are found in the more evolved units (e.g. U = 17 ppm in G2 and G4; Th = 36 ppm in G3).The Na_2O vs K_2O plot (Fig. 4) displays a broad negative correlations for the whole pluton, but with significant variation within individual units. This is a typical evolutionary trend for low-Ca granites (Breaks and Moore 1992).

Chondrite-normalized REE diagrams (Fig. 5) show moderate to pronounced negative Eu anomalies (0.20-0.001), moderately fractionated to flat LREE patterns (La_N/Sm_N = 2.68-0.61) and nearly flat to positive HREE patterns (Gd_N/Yb_N = 1.30-0.49); these characteristics are similar to those found in some highly fractionated A- and I-types granites. An inversion of the REE pattern that is typical of felsic magmas is observed: a decrease in LREE and an irregular HREE increase accompanying a general decrease in the total REE content associated to a deeper Eu/Eu* anomaly. The LREE and HREE show two different patterns, i.e., negative slopes for both G1 and G3 and flat or even positive slopes for G2 and G4
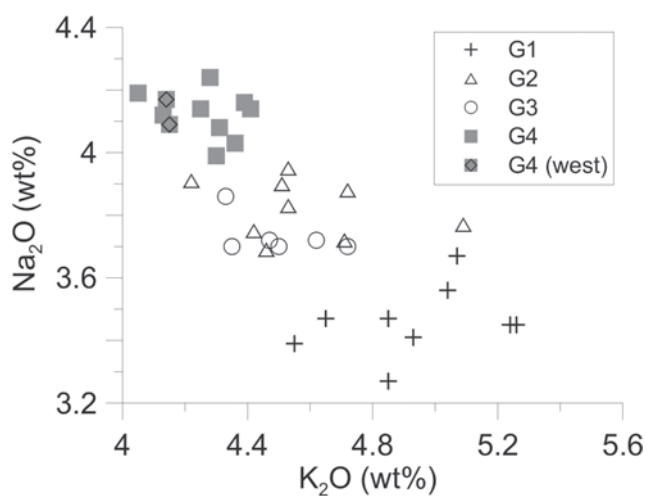
(e.g. sample 106045 of G4: La_N / Sm_N = 0.64 and Gd_N / Yb_N = 0.69). Flat REE patterns from G2 and G4 show the lanthanide tetrad effect in the third (Gd-Ho) and fourth (Er-Lu) tetrads, but is less accentuated in the first tetrad (La-Nd); this last is usually the most pronounced in felsic granites (Irber, 1999). A Pr negative anomaly in the most evolved La Pedriza units disturbs the first tetrad effect. The degree of the tetrad effect in the REE patterns, expressed by the factor $TE_{1,3}$ (Irber, 1999), ranges from 1-1.2 (Table 1), although the more poorly defined first tetrad (e.g. sample 105575: TE_1 = 1.04 versus TE_3 = 1,34) decreases the $TE_{1,3}$ mean. The contraction in the heavier elements of the fourth REE tetrad (Er-Lu) in the G4 granites is worthy of note (Fig. 5). The lanthanide tetrad effect described in the La Pedriza granites are not analytical artifacts (see electronic appendix on REE analytical procedures).

The bulk-crust normalized diagrams show similar patterns for all the La Pedriza leucogranites (Fig. 6). From the G1 to the G4 granites, progressively deeper negative anomalies for Ba, Sr, (La, Ce), Eu and Ti are observed. Similar trends have been described from some peralkaline A-type granites (e.g. Han et al., 1997) and fractionated I-type granites (e.g. Champion and Chappell, 1992).

The role of volatile and light elements (F, Li) in the La Pedriza leucogranites is not clear. In contrast to the good correlations found in other evolved granites (e.g. Dostal and Chatterjee, 1995), F contents are not clearly correlated with other incompatible elements (Fig. 7a); only G2 and G4 granites show a broad positive correlation with U contents (Fig. 7b). On the other hand, Li contents are clearly correlated with some incompatible elements, i.e. Rb, Cs and Ga (Fig. 7c) although some negative correlations with Nb, Ta, Y, HREE, Sn and Sc do occur in the G4 unit. Li contents decrease with those of compatible elements such as Zr, Th and LREE, although with a lesser rate, in G4 also (Fig. 7d).

Radiogenic isotopes

Sr and Nd isotopic analysis of the La Pedriza pluton units are listed in Table 3. Initial $^{87}Sr/^{86}Sr$ for G1 and G2 are low (0.7036-0.7065). The G3 and G4 granites are characterised by extremely high Rb/Sr reflecting extremely low Sr contents (<3 ppm) and very high Rb contents. Thus, as the initial ratios calculated are very sensitive to variation in the calculation age, unrealistic initial values ($\leq$0.700) were obtained. We have used as initial $^{87}Sr/^{86}Sr$ ratios for G3 and G4 granites in Figure 8, the whole-rock isochron IR of 0.7057 determined by Pérez-Soba (1992) (see also Table 3). All of the granites have negative $\varepsilon Nd_{(T)}$ values ranging from -6.59 to -4.04. The composition fields of other lithologies of the SCS (Villaseca et al. 1998; Bea et al., 1999) are shown in Figure 8. The studied leucogranites have isotopic compositions in the range of other I-type granites
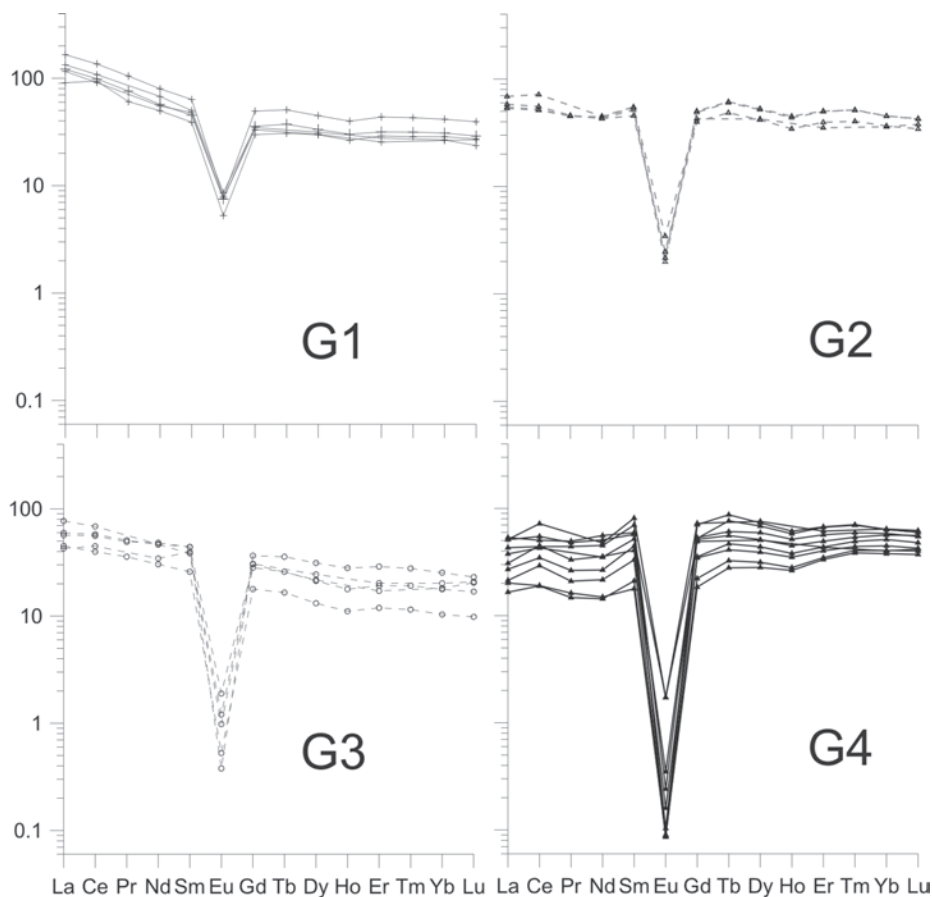

FIGURE 4 | **Correlation of Na_2O and K_2O in the four units of the La Pedriza leucogranites.**

FIGURE 5 | **Whole-rock, chondrite-normalized REE patterns for the units of the La Pedriza leucogranites and their different patterns. Note also the significant tetrad effect in the first- and third tetrad of the G2 and G4 unit. Normalization values are from Sun and McDonough (1989).**

from the SCS (Fig. 9), although with the lowest $^{87}Sr/^{86}Sr$ values. On the other hand, the granite with the highest Sr content (45 ppm, G1 unit) has the lowest initial $^{87}Sr/^{86}Sr$ ratio of all.

DISCUSSION

Alteration processes

Alteration in felsic granites make rock classification more difficult and petrogenetic conclusions problematical as alteration trends may be confused with those of magmatic processes (e.g. King et al., 1997). The La Pedriza leucogranites exhibit various late- to postmagmatic transformations. As was described above, each unit shows a characteristic alteration suggesting that the changes happened shortly after unit crystallization when pervasive post-magmatic alteration was unlikely. SHRIMP U-Pb ages of metamictic zircons from G4 do not show age differences with primary crystals, suggesting that the alteration occurred shortly after magmatic crystallization (Nasdala et al., 2009).

Plagioclase in the leucogranites is albite-rich, a criterion considered by some (King et al., 1997) as evidence of

alteration. It is suggested that lower CaO whole-rock contents (< 1 wt%) might be associated with albitization. In a CaO vs. Sr plot (Fig. 9a), the studied granites show some positive correlation. Moreover, if albitization were significantly developed, Sr (more sensitive to alteration) would have shown a detachment from this path. Metasomatic albitization is sometimes related to REE depletion (Zaraysky et al., 2007). However, such is not observed in any of the granite units (Fig. 9b).

Compositional changes due to alteration are considered to be minor as most of the samples show good correlations with typical magmatic fractionation indexes (e.g TiO_2, K/Rb). As the presence of volatile phases (see below) decreases the temperature of the magma solidus (e.g. Tuttle and Bowen, 1958; Pichavant and Manning, 1984; London, 1987), this could enhance late transformation, and support the conclusion that the pluton compositional variability mainly originated in an evolving magmatic system.

Fractional crystallization

The La Pedriza leucogranites are highly evolved magmas. The high Rb (< 629 ppm), and Sr and Ba contents as low as 1 ppm found in the most differentiated unit (G4)

indicate that crystal fractionation was likely the main process driving magma evolution. The Q-Ab-Or compositions and the limited ranges in SiO_2, Al_2O_3 and alkalis contents suggest that crystallization of the leucogranites occurred close to the minimun in the granite system (Christiansen et al., 1986). Significant ratios (Rb/Sr > 4.4, Ca/Sr > 113, Rb/Ba > 0.6, K/Ba > 113, Eu/Eu* < 0.2) in the G1 leucogranite suggest that earlier fractionation of K-feldspar and plagioclase was already significant in this least fractionated unit. As Zr/Hf also decreases with increasing evolution of a silicate melt (e.g. Irber, 1999), some authors have suggested this ratio as a granite fractionation index (Bea et al., 2006; Zaraysky et al., 2007). The La Pedriza leucogranites show Zr/Hf ratios characteristic of highly-evolved granites, (Zr/Hf = 28-10) and even lower than pegmatite averages (~25, Erlank et al., 1978). Villaseca et al. (1998) showed in a model that the evolution from a less-evolved G1 sample (EX-203) to the most evolved G4 granite required the averaged fractionation of 30% plagioclase, 30% quartz, 30% K-feldspar and 10% biotite.

The use of log-log plots involving elements of different geochemical behaviour can be used to identify fractional crystallization processes (Allègre and Minster, 1978). In some plots, the La Pedriza leucogranites do not define a single evolution line starting from the less evolved rocks of G1, although a rough general trend characterizes most major- and trace element plots. Feldspar fractionation is one of the clues in the evolution in highly felsic magmas. Log-plots involving Rb, Sr, Eu/Eu* and Ba illustrate the importance of K-feldspar and plagioclase fractionation, and of biotite. In Fig. 10a and b, a discontinuous trend reflecting a large decrease in Ba, Sr and Eu/Eu* and a relatively small increase of Rb is shown; the evolution of each unit seems to be controlled by different proportions of major minerals. The G1 and G2 units are characterized by short sequences of fractionations that are mainly controlled by K-feldspar and biotite. The G3 unit defines a trend which seems to depart from that of the G2 unit and parallels that of G4 but containing considerably less Rb (Fig. 10b) and displaying a less-marked Eu negative anomaly (Fig. 10a). G4 granites show a more extended degree of fractionation with K-feldspar controlling the variation of Sr, Ba and Eu, and Ab-rich plagioclase acting to deepen the Eu anomaly (Fig 10a). In the Q-Ab-Or diagram, the G4 granites shift the minimum towards the Ab vertex,
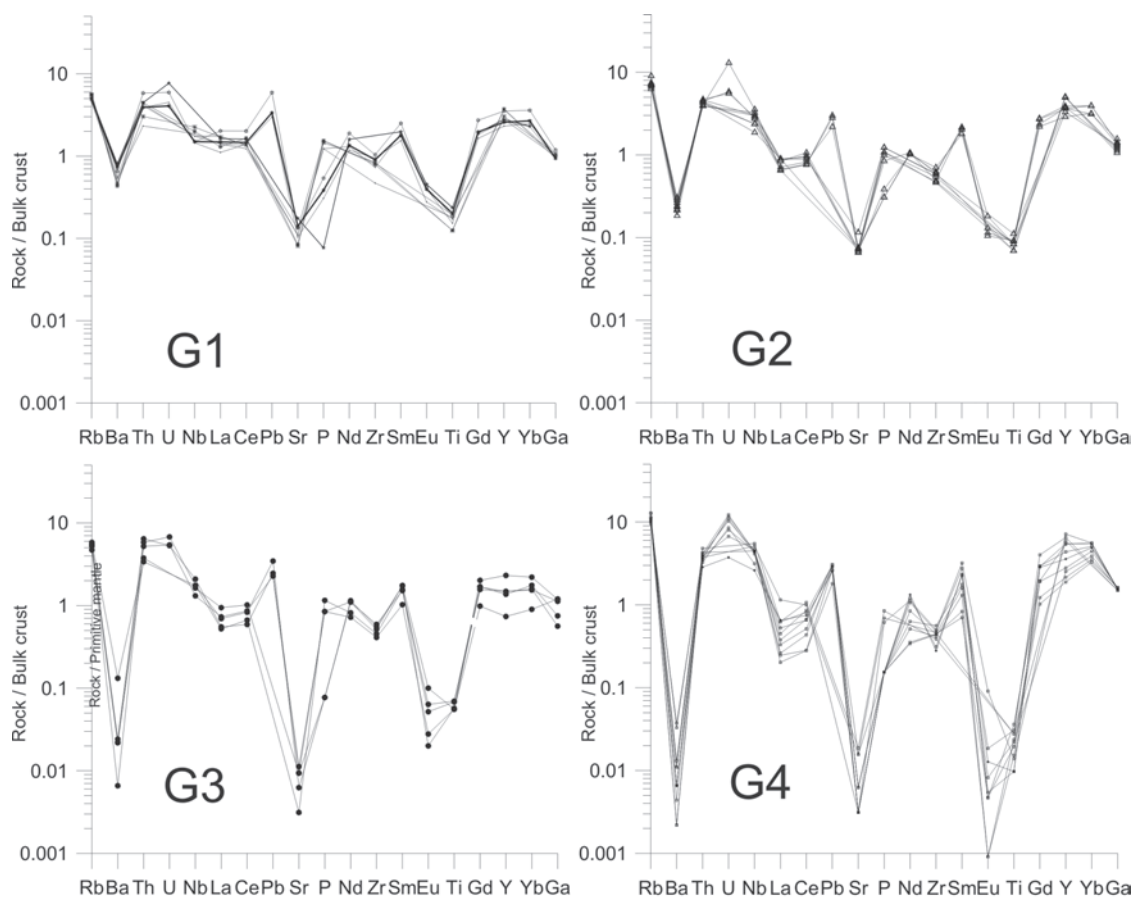

FIGURE 6 | **Bulk-crust-normalized trace element diagrams for the four units of the La Pedriza leucogranites. Note the marked anomalies in Ba, Sr, Eu and Ti. Normalization values are from Rudnick and Gao (2003).**
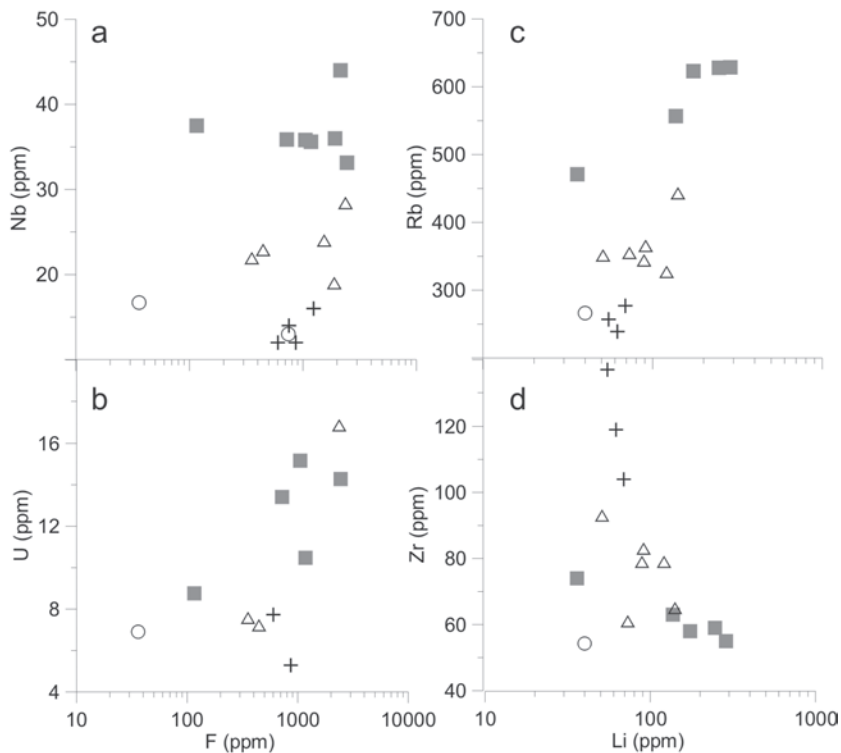
FIGURE 7 | **Variation diagrams of F and Li vs representative trace elements of the La Pedriza leucogranites. The samples of the G4 unit, in general, mark a change in the evolutionary paths of the trace elements and of the wider compositional range when compared to the other three units. a) Plot showing poor F vs. Nb correlations for the four units. b) Plot showing positive F vs U correlation that is unique to the G4 unit. c) Li vs Rb plot showing the incompatible behavior of both elements in the G4 unit. d) Li vs Zr plot exhibiting negative correlation for the G4 unit.**

which suggests a lesser involvement of K-feldspar and quartz in their fractional crystallization trend. A similar trend is experimentally explained by significant increases of F, Li or B contents in the magma (c.f. Mackenzie et al., 1988).

Variations in FeO, MnO, TiO_2, MgO, Sn, Cs, Li and F (and Rb and Ga) contents are explained mainly by biotite compositional changes. The estimated protolithionite composition of the biotite would involve an increase in Li, Cs, Rb and Mn contents and a progressive decrease in Fe, Ti and Mg (Tischendorf et al., 2001; Table 2, this paper). Fe-Ti oxides may contribute to the decreasing Fe, Ti and Mn trends in the four units. High oxygen fugacities attained in G3 would promote magnetite crystallization and favour tetra-ferri-annite composition in micas. This condition is indicated by the very low Sn values characterizing the G3 unit; high Sn contents may be used to indicate reduced magma conditions (Blevin and Chappell, 1992).

Variations in Zr, Hf, Y, REE, Nb, Ta and Sc in the La Pedriza leucogranites are consistent with the crystallization of accessory minerals and changes in their compositions. Different units show different trends, as illustrated by the spreading REE contents in G4 granites (56-150 ppm) compared to the short ranges shown by the G2 (118-126 ppm) and G3 granites (12-29 ppm). In Figure 3, Zr

contents decrease from G1 to G4, but each unit shows an independent trend characterized by a steeper slope than the general pattern. However, the less-evolved units (G1 and G3) do not show a clear variation of Zr with differentiation. Zircon fractionation controls the decreases in Zr and Hf and, together with the rare xenotime, also partly controls the HREE (Fig. 11a) and Y contents in the less evolved G1 and G3 units.

Xenotime crystallization is evaluated in the Y vs. HREE plot (Fig. 11b) which shows a positive correlation from G1 to G4. Nevertheless, if we consider the evolution of Y in each unit using Rb as a fractionation index (Fig. 11c), only in G1 are increases in both elements evident. In the other three units, and particularly in G4, decreasing trends suggest that xenotime fractionation occurred in each. In the G4 unit, with decreasing K/Rb ratios (i.e. fractionation), Gd_N / Yb_N and HREE contents decrease. Moreover, similar xenotime HREE and whole-rock patterns (including the third tetrad effect) suggest that xenotime fractionation is the main control on HREE in the G4 unit. The fact that xenotime in the G4 unit becomes progressively richer in the heaviest HREE (Yb, Lu) suggests that its fractionation would also explain the contraction in the fourth tetrad (Fig. 5). Nevertheless, the co-crystallization of other Y-bearing and/or other HREE-bearing accessory minerals (e.g. Y-columbite, U-pyrochlore and zircon) in the G4 unit could contribute
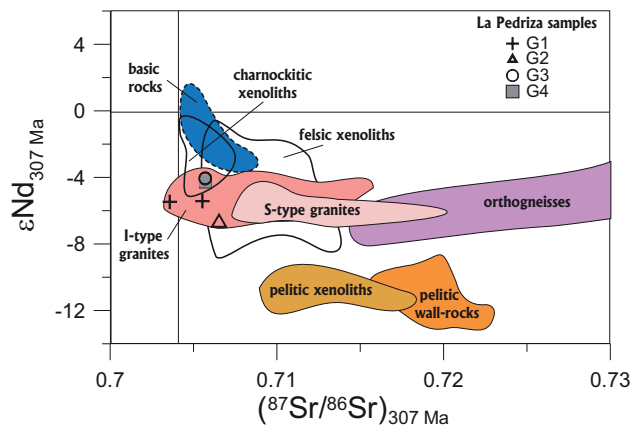
FIGURE 8 | $^{87}Sr/^{86}Sr$ vs. εNd diagram showing the isotopic composition of the La Pedriza leucogranites compared with other SCS compositional fields (Villaseca et al., 1998; Bea et al., 1999; Villaseca et al., 2007). All values have been recalculated to 307 Ma, the Rb-Sr isochron age of the La Pedriza pluton.

to variations in the decrease of HREE relative to Y during late crystallization.

Nb, Ta and Sc are controlled in the La Pedriza leucogranites mainly by niobotantalates. These elements are strongly partitioned in melts (London, 1987), reaching high concentrations in the most evolved granites. In terms of Rb content vs Nb or Ta or Sc (Fig. 11d and e), different characterizing variation trends stress the compositional contrast between the magma units. In G1, G2 and G3, Nb, Ta and Sc define increasing trends with fractionation whereas, with the exception of two samples from the western sector, these elements define a slope with a decreasing trend in G4 (Fig. 11e); niobotantalate precipitation during the G4 evolution is indicated.

Though La and Nd contents decrease in all units with magmatic differentiation, they describe a different, longer and steeper evolutionary trend in G1 and G3 when compared with the other two more evolved units (Fig. 11f). These patterns suggest that monazite fractionates in the whole magmatic suite but in differing proportions.

The P-poor magma composition determines the rare early crystallization of phosphates and, thus, favours an increasing richness in those incompatible elements usually incorporated into phosphate accessories (i.e. monazite, xenotime and apatite) in residual magma (Bea, 1996). Monazite and zircon fractionate in all of the units, xenotime in G2, G3 and G4, whereas niobotantalates fractionates only in G4. This last unit is characterized by the absence of allanite, the scarcity of monazite, zircon rich in Y-HREE and the elevated abundance of xenotime and niobotantalates. Although G4 granites have the highest Y-HREE-Nb-Ta-Sc contents, these elements decrease as feldspar and accessory-mineral fractionation continues. That this trend is also related to the coeval crystallization of Li-rich trioctahedral micas (protolithionite mica) is suggested by the good correlations of Li with FeO and MgO contents.

Role of volatiles

A F-rich phase will significantly influence magma liquidus and solidus temperatures, the viscosity of silicate melts, the sequence of mineral crystallization, the partitioning of trace elements and the extent of fractional crystallization (e.g. Manning, 1981; Černy et al., 1985; London, 1987; Mackenzie et al., 1988; Keppler, 1993; Webster and Rebbert, 1998; Dingwell et al., 1998). Indeed, in highly-evolved granitic melts, the control of element distribution between mineral and melt may be conditioned by chemical complexing with different ligands in aqueous systems if a fluid phase is exsolved (Collins et al., 1982, Irber, 1999; Bau, 1997; Dostal and Chatterjee, 2000). However, Xiaolin et al. (1998) suggest that F is concentrated in granitic melt relative to a coexisting fluid, and that this feature is more evident in low-F granite magmas.

The following criteria have been used for discussing the involvement of volatile components in residual granitic melts:

1) Low K/Rb in felsic granites (< 150, Irber, 1999; < 100, Clarke, 1992) is regarded as evidence of interaction with an aqueous fluid phase (Clarke, 1992; Irber, 1999; Dostal and Chatterjee, 1995) or of mineral growth in the

TABLE 3 | Sr and Nd isotopic composition of the La Pedriza leucogranites

Unit	Sample	Rb (ppm)	Sr (ppm)	$^{87}Rb/^{86}Sr$	$^{87}Sr/^{86}Sr$	±2σ	$(^{87}Sr/^{86}Sr)_t$	Sm (ppm)	Nd (ppm)	$^{147}Sm/^{144}Nd$	$^{143}Nd/^{144}Nd$	±2σ	$\varepsilon Nd_{(t)}$
G1	68931	257	43	19.36	0.79007	5	0.705534	9.76	37.8	0.1561	0.512278	5	-5.43
G1	87225	239	45	16.74	0.77674	6	0.703574	6.98	27.5	0.1563	0.512276	6	-5.47
G2	87161	327	23	44.1	0.89925	7	0.70653	8.45	21.32	0.2396	0.512387	6	-6.59
G3	106046	231	2.5	297	1.84178	13	0.7057*	5.92	22	0.1627	0.512363	5	-4.04
G3	107031	255	2	466	3.39607	88	0.7057*	6.78	22.9	0.179	0.512393	5	-4.08
G4	106045	629	1	1694	n.d.		0.7057*	5.1	10.24	0.3023	0.512634	5	-4.21

*An initial $^{87}Sr/^{86}Sr$ value of 0.7057 taken from the Rb-Sr whole-rock isochron of Pérez-Soba (1992) has been considered as representative for these high Rb/Sr granites (see text for further explanation). n.d. = not determined. Initial isotope ratios of granites are recalculated to 307 Ma, the supposed intrusion age of the pluton (Pérez-Soba, 1992).
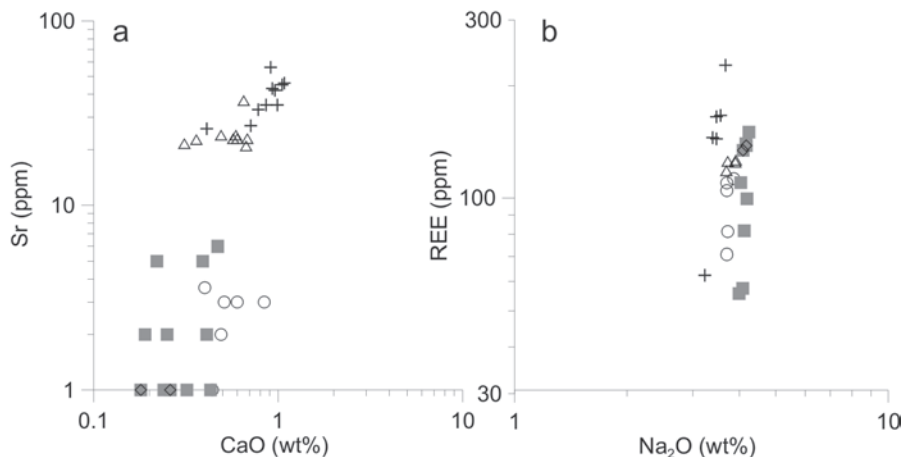
FIGURE 9 | a) CaO *vs.* Sr and b) Na$_2$O vs. REE log-log variation diagrams for the La Pedriza leucogranites. Same symbols as in Figure 3.

of aqueous fluids (e.g., Shearer et al., 1985). Nevertheless, the K/Rb of the most fractionated G4 and G2 leucogranites (<70 and < 123, respectively) point mainly to an extended feldspar fractionation process. The relatively high contents of F (< 2444 ppm) in the G4 unit would suggest the progressive influence of F-bearing phases (e.g., fluorine) in the late-stage evolution of the La Pedriza granitic magmas, in agreement with experiment (Xiaolin et al. 1998).

2) Fluorite crystallized interstitially together with trioctahedrical micas and other accessory minerals rich in HFS elements or with Ab-rich plagioclase. These textural features suggest the parallel enrichment of F and HFS elements in the residual magmas. Indeed, in the G2 and G4 leucogranites, F shows good correlations with Li, Cs, Rb, Sn, Ti, Fe and Ga. F (and Li) would favour late crystallization of siderophyllite to protolithionite; lithium micas are rich in Rb, Cs and F (Förster et al., 2005). On the other hand, F shows poor correlations with other incompatible elements, (e.g., Y, REE, Nb, Ta) that are mainly controlled by accessory minerals. This behaviour could reflect i) F crystallizing as fluorite and not being incorporated into other late-magmatic accessories, ii) very late concentration of F after accessory-mineral precipitation or iii) the partial and irregular loss by degassing of some of the original F (Taylor, 1992) with the result that measured contents do not relate to original magmatic contents (Qiu et al., 2004). In the G4 unit, F was remobilized during local subsolidus alteration, e.g., during bastnaesite formation.

3) G2 and G4 leucogranites show a moderate but significant lanthanide tetrad effect (TE$_{1,3}$ = 1.09-1.22), especially in the third tetrad (Fig. 5), as has been widely documented as evidence for the involvement of a volatile-rich fluid in the last stage of granite crystallization (see Janh et al., 2001). Bau (1996) proposed that good correlations of TE$_{1-3}$ with some pairs of elements (K/Rb, Zr/Hf, Sr/Eu,

Eu/Eu* and Y/Ho) were evidence of fluid interaction during the final stages of magma differentiation. In the La Pedriza leucogranites, good correlations are only shown by some ratios, e.g., Sr/Eu in Fig. 12. This correlation is not shown by Y/Ho and F. Although richness of fluorine is the
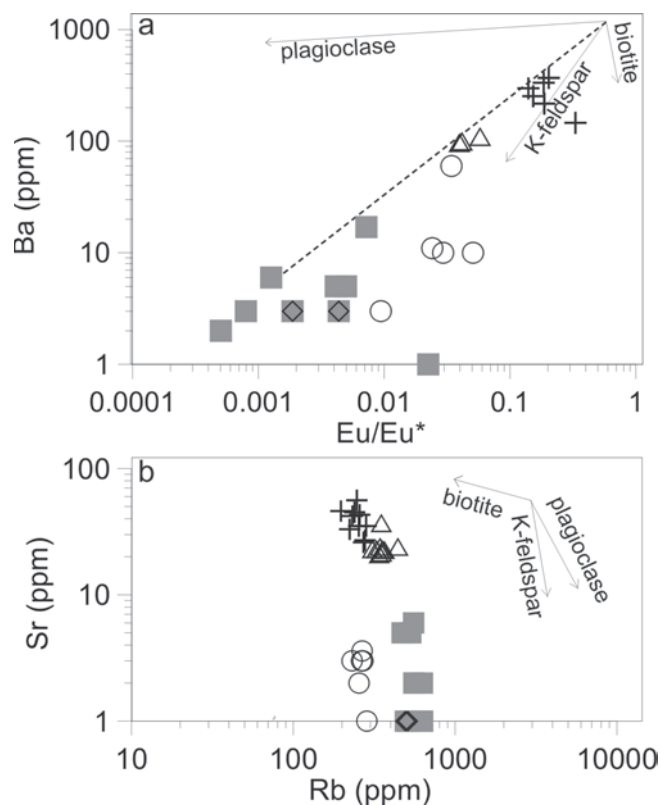

FIGURE 10 | a) Rb *vs.* Sr and b) Eu/Eu* vs. Ba – log-log diagrams that indicate the role of rock-forming minerals in the fractional crystallization. In a) vectors of fractional crystallization for K-feldspar, plagioclase and biotite are after Breaks and Moore (1992), and in b) from Landerberger and Collins (1996). Same symbols as in Figure 3.
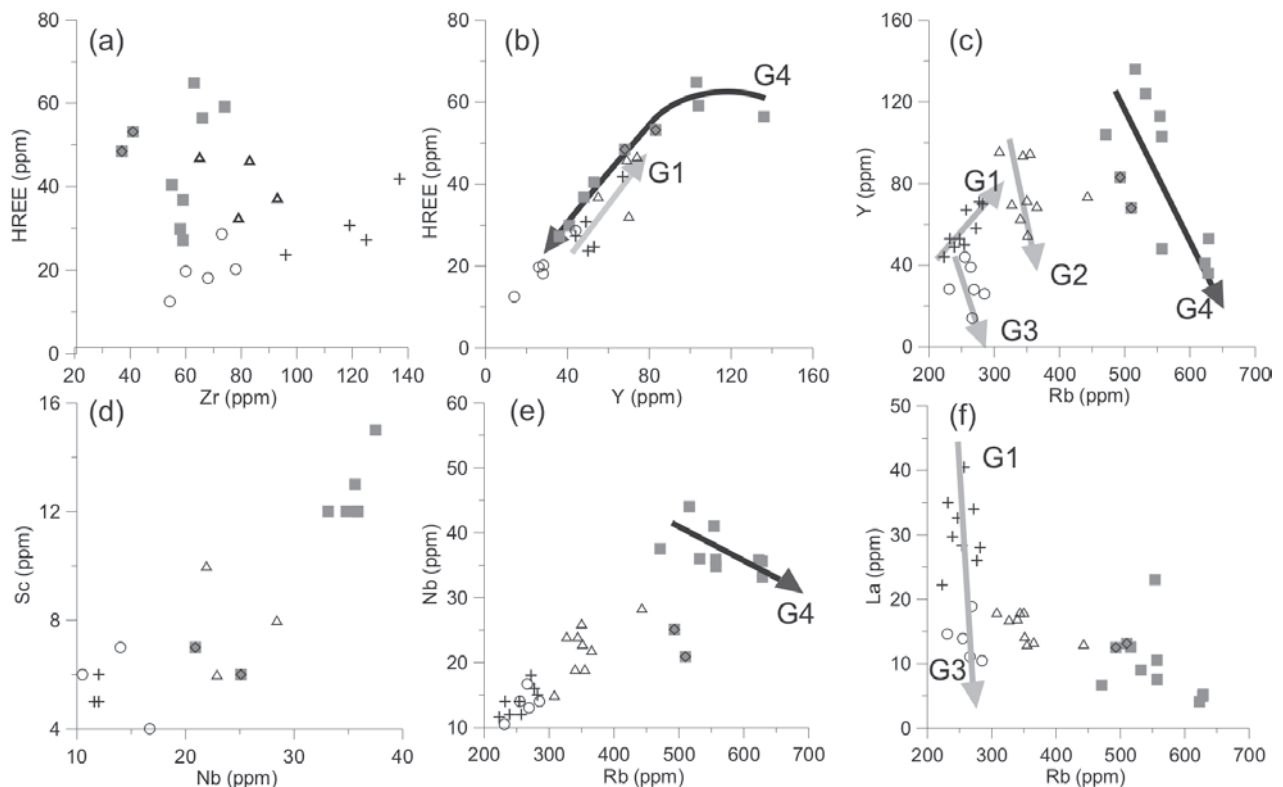
FIGURE 11 | **Variation diagrams for some trace elements as indicators of the evolution of the main accessory minerals in the La Pedriza leucogranites. a) Zr vs. HREE plot for zircon, b) Y vs. HREE and c) Rb vs. Y for xenotime, d) Nb vs Sc and e) Rb vs. Nb for niobiotantalites, f) Rb vs. La for monazite. Arrows on evolutionary trend lines indicate differentiation trends. Same symbols as in Figure 3.**

necessary condition for the development of the TE_{1-3} effect, not all F-rich granites show the effect, e.g., the peralkaline A-type granites of SE China (Qiu et al., 2004).

4) A complex paragenesis of Na-Li-rich amphiboles characterizes discrete alkaline episyenite bodies cropping out some meters from the northeastern contact of the G4 unit (Caballero et al., 2002; Villaseca and Pérez-Soba, 1989). In addition, some greisens occur locally in the northeastern margin of the G4 unit. A possible genetic link between the episyenites and volatile exsolution from G4 requires further study.

Granite type assignation

Owing to extended fractional crystallization, the La Pedriza leucogranites show the compositional and mineralogical features of fractionated A- and I-type granites. A wide compositional range would have provided a more reliable classification as low-silica rocks reveal the type assignation more clearly. However, the most primitive La Pedriza sample is already a silica-rich granite (72.7 wt% SiO_2). Many of the discrimination diagrams in the literature involve trace elements (Ga, Y/Nb, Ce/Nb, Sc, etc.) which are not reliable for

the classification of highly evolved granites as their abundances are mainly controlled by accessory minerals. Trace element contents increase with fractionation without any relation to their concentrations in the parent magma (Landerberger and Collins, 1996). Chemical parameters which include trace elements controlled by different accessory minerals, e.g., Zr+Nb+Ce+Y, may mislead. With these limitations in mind, some diagrams that allow comparison with well characterized A-type granites are used below.

The La Pedriza leucogranites have SiO_2 contents in the range of 73-78 wt%. For that range, their chemistry is similar to that of A-types granites; they are characterized by high Fe/Mg (< 173), Na_2O+K_2O (8-8.9 wt%), Nb (< 44 ppm), Ga (< 26 ppm) and Y (< 136 ppm). The La Pedriza leucogranites show that some HFSE contents, e.g., Ga, Zr and Nb, increase with fractionation from baseline levels typical of I-type granites – as is also the case with other granites rich in rare metals (Champion and Chappell, 1992). The 1000Ga/Al vs. Zr or Zr+Nb+Ce+Y plots (Fig. 13) show that primitive La Pedriza leucogranites clearly fall outside the A-type compositional field and that their most fractionated units (G2-G4) have values clearly below those of typical A-type granite suites.
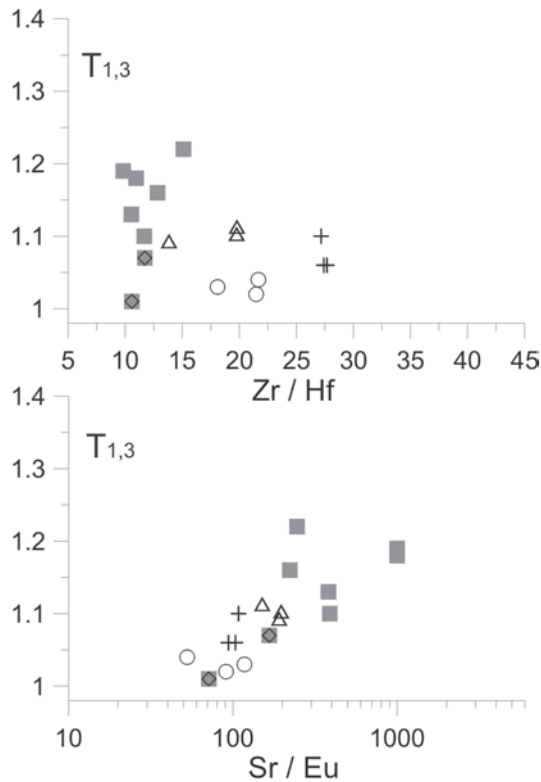
FIGURE 12 | **a) Tetrad effect (TE$_{1-3}$ of Irber 1999) vs. Sr/Eu and b) Zr/Hf as indicators of the granite differentiation. Same symbols as in Figure 3.**

Granite sources

Derivation from magmas of mantle origin has been proposed for some I-type granites (see King et al., 1997). Others consider it unlikely that highly felsic granites can be derived from basaltic rocks by fractionation (e.g., Champion and Chappell, 1992; King et al., 1997).

It has been suggested that the availability of crustal felsic rocks during the anatexis could explain the typical geochemistry of some A-type granite magmas (e.g., Clemens et al., 1986; Skjerlie and Johnston, 1993; Landerberger and Collins, 1996). Indeed, Patiño Douce and Harris (1998) consider that peraluminous leucogranite magmas are probably derived by melting of the continental crust without contamination of a mantle component. The initial εNd values of the La Pedriza leucogranites (Table 3) suggest that they were derived from continental crustal sources rather than from a long-term depleted mantle. Villaseca et al. (1999, 2007) consider that granulite xenoliths in upper Permian alkaline lamprophyre dikes could represent the residual composition of the lower crust after production of the voluminous Hercynian SCS batholith. The most abundant felsic, peraluminous, granulite-type xenoliths (95 vol% of the xenolith suite) are related to the origin of the dominant peraluminous granites in the SCS batholith. The rare mafic- and metaluminous charnockite granulites (ca 1 vol% of the xenolith suite) better match the Sr-Nd isotopic composition of the less peraluminous, SCS, I-type granites, e.g., the La Pedriza granite. The granulite-granite genetic link is supported by similar age ranges (310-285 Ma; Fernández-Suárez et al., 2006), and by isotopic (Sr-Nd-O), major- and trace element compositions (Villaseca et al., 1999, Villaseca & Herreros, 2000).

Frindta et al. (2004) consider that, for evolved granites, radiogenic isotopic ratios are the main criterion for discussion of magma sources. As evident in Figure 8, G3 and G4 have initial Nd isotopic compositions (εNd = -4 to -4.2) that lie within the SCS charnockite granulite composition field (εNd = −1 to –4.3), whereas G1 and G2 have similar εNd ranges to the other SCS felsic granulite xenoliths. All of the La Pedriza leucogranites clearly lie
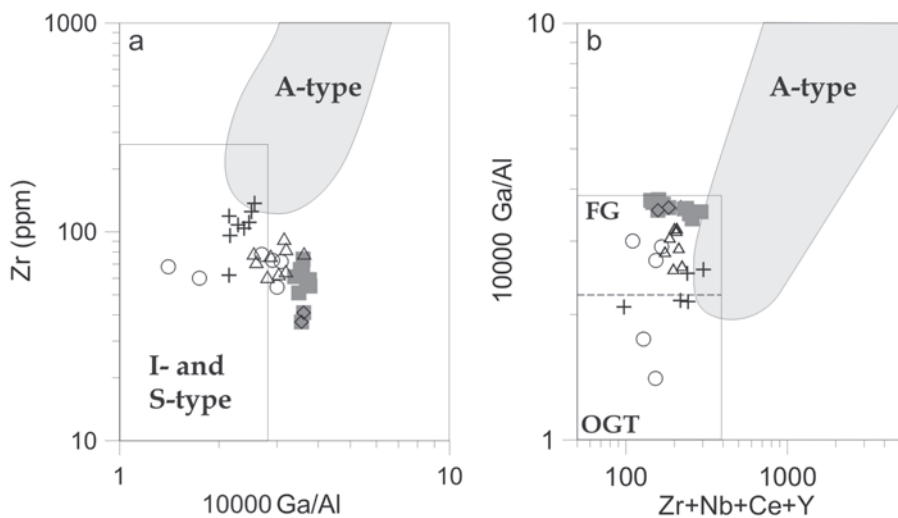

FIGURE 13 | **a) 10000 Ga/Al vs. Zr discrimination diagram (after Whalen et al., 1987). b) Zr+Nb+Ce+Y vs 10000 Ga/Al plot (Whalen et al., 1987). OGT (unfractionated M-, I- and S-type granites) and FG (fractionated felsic granites) fields taken from Whalen et al. 1987. A-type granite compositional field taken from Eby (1990). Same symbols as in Figure 3.**

below the Nd isotopic composition of the SCS basic rocks. The absence of coeval mafic magmas and the lack of isotopic mixing lines between basic rocks and suitable crustal rocks, essentially rule out basic rocks as a major component in the La Pedriza magmas. We consider the partial melting of intermediate meta-igneous granulites to be a more plausible model. Kostitsyn (2001) and Kostitsyn et al. (2007) have proposed that the anatectic melting of a crustal source could explain high concentrations of many lithophile elements in similar I-type, Li-F granites. In addition, F and rare-metal enrichment most probably results from the fractional crystallization of these granitic melts.

CONCLUSIONS

The four main intrusive units of the La Pedriza pluton cryptically define a granite suite that does not reflect a simple crystal fractionation process; chemical diagrams show compositional gaps, markedly different trends and singular REE chondrite normalized patterns for each. These trends are interpreted as changes in the distribution coefficients of the major phases, different degrees of fractionation and different accessory mineral populations - all influenced by the minimum-melt composition and, in the more evolved units, late-stage volatile enrichment.

As with high-silica magmatic systems constructed by the successive accumulation of reduced magma volumes (Christiansen et al. 1986, Christiansen and McCurry 2008), the La Pedriza pluton comprise magma batches of different geochemical sources. The low convective capacity of the high-silica magma chamber inhibited homogenization, resulting in pulses characterized by significant isotopic differences. Fractional crystallization increased the original differences between the magmas. The G2 and G4 units display a nearly spatial concentric disposition but the different initial Nd isotopic ratios, the gaps in most of the major- and trace elements and the marked change in Sr content preclude the possibility of in-situ fractionation in a zoned magma chamber.

The most differentiated granite units of the La Pedriza pluton show high incompatible-element contents similar to those of A-types granitoids. We consider that the La Pedriza pluton evolved by fractional crystallization from a typical, I-type magma to one highly enriched in HFSE with the minor involvement, in the late stages, of F-rich residual melt. The characteristic P-poor composition of I-type magmas considerably accentuates the incompatible behavior of elements such as Th, U, Y and REE that are mainly controlled by P-rich accessory minerals. Nevertheless, the La Pedriza pluton cannot be considered a F-rich granite.

REFERENCES

Allègre, C.J., Minster, J.F., 1978. Quantitative models of trace element behaviour in magmatic process. Earth and Planetary Science Letters, 38, 1-25.

Barbero, L., Villaseca, C., 2000. Eclogite facies relics in metabasites from the Sierra de Guadarrama (Spanish Central System): P-T estimations and implications for the Hercynian evolution. Mineralogical Magazine, 64, 815-836.

Bau, M., 1996. Controls on the fractionation of isovalent trace elements in magmatic and aqueous systems: evidence from Y/Ho, Zr/Hf, and lanthanide tetrad effect. Contributions to Mineralogy and Petrology, 123, 323-333.

Bau, M., 1997. The lanthanide tetrad effect in highly evolved felsic igneous rocks - a reply to the comment by Y. Pan. Contributions to Mineralogy and Petrology, 128, 409-412.

Bea, F., 1996. Residence of REE, Y, Th and U in granites and crustal protoliths; Implications for the chemistry of crustal melts. Journal of Petrology, 37, 521-552.

Bea, F., Montero, P., Molina, J.F., 1999. Mafic precursors, peraluminous granitoids, and late lamprophyres in the Ávila batholith: A model for the generation of Variscan batholiths in Iberia. Journal of Geology, 107, 399-419.

Bea, F., Montero, P., Ortega, M., 2006. A LA-ICPMS evaluation of Zr reservoirs in common crustal rocks: implications for a Zr and Hf geochemistry, and zircon-forming processes. Canadian Mineralogist, 44, 693-714.

Bea, F., Montero, P., Zinger, T., 2003. The nature and origin of the granite source layer of Central Iberia: Evidence from trace element, Sr and Nd isotopes, and zircon age patterns. Journal of Geology, 111, 579-595.

Blevin, P.L., Chappell, B.W., 1992. The role of magma sources, oxidation states and fractionation in determining the granite metallogeny of eastern Australia. Transactions of the Royal Society of Edinburgh: Earth Sciences, 83, 305-316.

Brandebourger, E., 1984. Les granitoïdes hercyniens latefs de la Sierra de Guadarrama (Système Central, Espagne) Pétrographie et Géochimie. Doctoral Thesis. L´Institut National Polytechnique de Lorraine, 209pp.

Breaks, F.W., Moore, J.M., 1992. The Ghost Lake batholith, Superior Province of northwestern Ontario: a fertile, S-type,

peraluminous granite-rare-element pegmatite system. The Canadian Mineralogist, 30, 835-876.

Caballero, J.M., Oberti, R., Ottolini, L., 2002. Ferripedrizite, a new monoclinic BLi amphibole endmember from the Eastern Pedriza Massif, Sierra de Guadarrama, Spain, and a restatement of the nomenclature of the Mg-Fe-Mn-Li amphiboles. American Mineralogist, 87, 976-982.

Casillas, R., Nagy, G., Pantó, G., Brändle, J.L., Fórizs, I., 1995. Occurrence of Th, U, Y, Zr, and REE-bearing accessory minerals in late-Variscan granitic rocks from the Sierra de Guadarrama (Spain). European Journal of Mineralogy, 7, 989-1006.

Castiñeiras, P., Villaseca, C., Barbero, L., Martín Romera, C., 2008. SHRIMP zircon dating of anatexis in high-grade migmatite complexes of central Spain: implications in the Hercynian evolution of the Central Iberia. International Journal of Earth Sciences, 97, 35-50.

Cěrny, P., Meintzer, R.E., Anderson, A.J., 1985. Extreme fractionation in rare-element granitic pegmatites: selected examples of data and mechanisms. The Canadian Mineralogist, 23, 381-421.

Champion, D.C., Chappell, B.W., 1992. Petrogenesis of felsic I-type granites: an example from northern Queensland. Transactions of the Royal Society of Edinburgh: Earth Sciences, 83, 115-126.

Chappell, B.W., White, A.J.R., 1992. I- and S-type granites in the Lachlan Fold Belt. Transactions of the Royal Society of Edinburgh: Earth Sciences, 83, 1-26.

Christiansen, E.H., Sheridan, M.F., Burt, D.M., 1986. The geology and geochemistry of Cenozoic topaz rhyolites from the Western United States. Geological Society of America, 205(Special Paper), 1-82.

Christiansen, E.H., McCurry, M., 2008. Contrasting origins of Cenozoic silicic volcanic rocks from the western Cordillera of the United States. Bulletin of Volcanology, 70, 251-267.

Clarke, D.B., 1992. Granitoid Rocks. New York, Chapman and Hall, 283pp.

Clemens, J., Holloway, J.R., White, A.J.R., 1986. Origin of an A-type granite: experimental constraints. American Mineralogist, 71, 317-324.

Collins, W.J., Beams, S.D., White, A.J.R., Chappell, B.W., 1982. Nature and origin of A-type granites with particular reference to Southeastern Australia. Contributions to Mineralogy and Petrology, 80, 189-200.

Dingwell, D.B., Hess, K.U., Romano, C., 1998. Viscosity data for hydrous peraluminous granitic melts: comparison with the metaluminous model. American Mineralogist, 83, 236-239.

Doblas, M., Oyarzum, R., Sopeña, A., López-Ruiz, J.M., Capote, R., Hernández-Enrile, J.L., Hoyos, M., Lunar, R., Sánchez-Moya, Y., 1994. Variscan-late Variscan-early Alpine progressive extensional collapse of central Spain. Geodinamica Acta, 7, 1-14.

Dostal, J., Chatterjee, A.K., 1995. Origin of topaz-bearing and related peraluminous granites of the late Devonian Davis Lake pluton, Nova Scotia, Canada: crystal versus fluid fractionation. Chemical Geology, 123, 67-88.

Dostal, J., Chatterjee, A.K., 2000. Contrasting behavior of Nb/Ta and Zr/Hf ratios in a peraluminous granitic pluton (Nova Scotia, Canada). Chemical Geology, 163, 207-218.

Eby, G.N., 1990. The A-type granitoids: A review of their occurrence and chemical characteristics and speculations on their petrogenesis. Lithos, 26, 115-134.

Erlank, A.J., Marchant, J.W., Cardoso, M.P., Ahrens, L.H., 1978. Zirconium. Abundance in rock forming minerals, phase equilibria, zirconium minerals. In: Wedepohl, K.H. (ed.). Handbook of Geochemistry. New York, Springer Verlag-, II/4, 40-51.

Escuder Viruete, J., Hernáiz Huerta, P.P., Valverde-Vaquero, P., Rodriguez Fernández, R., Dunning, G., 1998. Variscan syncollisional extension in the Iberian Massif: structural, metamorphic and geochronological evidence from the Somosierra sector of the Sierra de Guadarrama (Central Iberian Zone, Spain). Tectonophysics, 290, 87-109.

Fernández-Suárez, J., Jeffreis, T.E., Whitehouse, M.J., Arenas, R., Villaseca, C., 2006. A U-Pb geochronological study of zircons from lower crustal granulite xenoliths of the Spanish Central System: a record of Iberian lithospheric evolution from the Neoproterozoic to the Triassic. Journal of Geology, 114, 471-483.

Förster, H.J., Tischendorf, G., Rhede, D., Naumann, R., Gottesmann, B., Lange, W., 2005. Cs-rich lithium micas and Mn-rich lithian siderophyllite in miarolitic NYF pegmatites of the Königshain granite, Lausitz, Germany. Neues Jahrbuch für Mineralogie - Abhandlungen, 182, 81-93.

Frindta, S., Trumbull, R.B., Romer, R.L., 2004. Petrogenesis of the Gross Spitzkoppe topaz granite, central western Namibia: a geochemical and Nd-Sr-Pb isotope study. Chemical Geology, 206, 43-71.

González del Tánago, J., Pérez-Soba, C., Villaseca, C., 2004. Minerales accesorios de Nb-Ta-Ti e Y-REE-Th-U en el plutón granítico de La Pedriza, Sistema Central Español. Geotemas, 6, 57-60.

Han, B.F., Wang, S.G., Jahn, B.M., Hong, D.W., Kagami, H., Sun, Y.L.B., 1997. Depleted-mantle source for the Ulungur River A-type granites from North Xinjiang, China: geochemistry and Nd-Sr isotopic evidence, and implications for Phanerozoic crustal growth. Chemical Geology, 138, 135-159.

Iber, W., 1999. The lanthanide tetrad effect and its correlation with K/Rb, Eu/Eu*, Sr/Eu, Y/Ho, and Zr/Hf of evolving peraluminous granite suites. Geochimica et Cosmochimica Acta, 63, 489-508.

Jacobsen, S.B., Wasserburg, G.J., 1980. Sm-Nd isotope evolution of chondrites. Earth and Planetary Science Letter, 50, 139-155.

Jahn, B., Wu, F., Capdevila, R., Martineau, F., Zhao, Z. and Wang, Y., 2001. Highly evolved juvenile granites with tetrad REE patterns: the Woduhe and Baerzhe granites from the Great Xing'an Mountains in NE China. Lithos, 59, 171-198.

Keppler, H., 1993. Influence of fluorine on the enrichment of high field strength trace elements in granitic rocks. Contributions to Mineralogy and Petrology, 114, 479-488.

King, P.L., White, A.J.R., Chappell, B.W., Allen, C.M., 1997. Characterization and origin of aluminous A-type granites from the Lachland Fold Belt, Southeastern Australia. Journal of Petrology, 38, 371-391.

King, P.L., Chappell, B.W., Allen, C.M., White, A.J.R., 2001. Are A-type granites the high-temperature felsic granites? Evidence from fractionated granites of the Wangrah Suite. Australian Journal of Earth Sciences, 48, 501-514.

Kostitsyn, Y.A., 2001. Sources of rare metals in peraluminous granites: a review of geochemical and isotopic data. Geochemistry International, 39, 43-59.

Kostitsyn, Y.A., Belousova, E.A., Volkov, V.N., 2007. Significance of magma fractionation in generation of rare-metal granites: geochronolgical and geochemical study of the Raumid multiphase granite (S. Pamir). Stellenbosch University (South Africa), Sixth International Hutton Symposium, Abstract volume, 108-109.

Kretz, R., 1983. Symbols for rock-forming minerals. American Mineralogist, 68, 277-279.

Landerberger, B., Collins, W.J., 1996. Derivation of A-type granites from a dehydrated charnockitic lower crust: evidence from the Chaelundi Complex, Eastern Australia. Journal of Petrology, 37, 145-170.

Loiselle, M.C., Wones, D.R., 1979. Characteristics and origin of anorogenic granites. Geological Society of America Bulletin, 11(Abstract), 468.

London, D., 1987. Internal differentiation of rare-element pegmatites: effects of boron, phosphorus, and fluorine. Geochimica et Cosmochimica Acta, 51, 403-420.

MacKenzie, D.E., Black, L.P., Sun, S., 1988. Origin of alkali-feldspar granites: An example from the Poimena Granite, northeastern Tasmania, Australia. Geochimica et Cosmochimica Acta, 52, 2507-2524.

Manning, D.A.C., 1981. The effect of fluorine on liquidus phase relationships in the system Qz-Ab-Qr with excess water. Contributions to Mineralogy and Petrology, 76, 206-215.

Martin, R.F., 2007. The petrogenesis of A-type granites: A fresh look outside the box. Stellenbosch University (South Africa), Sixth International Hutton Symposium, Abstract volume, 131-132.

Montero, P., Bea, F., Zinger, T.F., Scarrow, J.H., Molina, J.F., Whitehouse, M.J., 2004. 55 million years of continuous anatexis in Central Iberia: Single zircon dating of the Peña Negra Complex. Journal of the Geological Society, 161, 255-264.

Nasdala, L., Kronz, A., Wirth, R., Váczi, T., Pérez-Soba, C., Willner, A., Kennedy, K., 2009. The phenomenon of deficient electron microprobe totals. Geochimica et Cosmochimica Acta, 73, 1637-1650.

Patiño Douce, A.E., Harris, N., 1998. Experimental constraints on Himalayan anatexis. Journal of Petrology, 39, 689-710.

Pérez-Soba, C., 1992. Petrología y geoquímica del macizo granítico de La Pedriza, Sistema Central Español. Doctoral Thesis. Madrid, Universidad Complutense de Madrid, 222pp.

Pérez-Soba, C., Reyes J., Villaseca C., 2001. El leucogranito de grano grueso de La Pedriza: un caso de criptozonación y fraccionamiento extremo en la Sierra de Guadarrama. In: Lago, M., Arranz, E., Galé, C. (eds.). Zaragoza, III Congreso Ibérico de Geoquímica, 405-409.

Pérez-Soba, C., Villaseca, C., González del Tánago, J., Nasdala, L., 2007. The composition of zircon in the peraluminous Hercynian granites of the Spanish Central System batholith. The Canadian Mineralogist, 45, 509-527.

Pichavant, M., Manning, D., 1984. Petrogenesis of tourmaline granites and topaz granites; the contribution of experimental data. Physics of the Earth and Planetary Interiors, 35, 31-50.

Qiu, J.S., McInnes, B.I.A., Xu, X.S., Allen, C.M., 2004. Zircon ELA-ICPMS dating for Wuliting pluton at Dajishan, southern Jiangxi and new recognition about its relationship to Tungsten mineralization. Geology Review, 50, 125-133.

Reyes, J., Villaseca, C., Barbero, L., Quejido, A.J., Santos, J.F., 1997. Descripción de un método de separación de Rb, Sr y Nd en rocas silicatadas para estudios isotópicos. Congreso Ibérico de Geoquímica I, 46-55.

Rudnick, R.L., Gao, S., 2003. The Composition of the continental crust. In: Holland, H.D. and Turekian, K.K. (eds.). The Crust. Oxford, Elsevier-Pergamon, Treatise on Geochemistry, R.L. Rudnick, 3, 1-64.

Sánchez-Muñoz, L., López Andrés, S., Fernández Hernán, M., García Guinea, J.L., 1990. Feldspatos de pegmatitas de clase II y IV en el área de Colmenar Viejo - Manzanares (Madrid). Boletín de la Sociedad Española de Mineralogía, 13, 155-168.

Shearer, C.K., Papike, J.J., Laul, J.C., 1985. Chemistry of potassium feldspars from three zoned pegmatites, Black Hills, South Dakota: implications concerning pegmatite evolution. Geochimica et Cosmochimica Acta, 49, 663-673.

Skjerlie, K.P., Johnston, A.D., 1993. Fluid-absent melting behaviour of an F-rich tonalitic gneiss at mid-crustal pressures: Implications for the generation of anorogenic granites. Journal of Petrology, 34, 785-815.

Sun, S.S., McDonough, W.F., 1989. Chemical and isotopic systematics of oceanic basalts; implications for mantle composition and processes. In: Saunders, A.D., Norry, M.J. (eds.). Magmatism in the ocean basins. London, Geological Society of London, 42 (Special Paper), 313-345.

Taylor, R.P., 1992. Petrological and geochemical characteristics of the Pleasant Ridge zinnwaldite-topaz granite, southern New Brunswick and comparisons with other topaz bearing felsic rocks. The Canadian Mineralogist, 30, 895-921.

Tischendorf, G., Gottesmann, B., Förster, H.J., Trumbull, R.B., 1997. On Li-bearing micas: Estimating Li from electron microprobe analyses and an improved diagram for graphical representation. Mineralogical Magazine, 61, 809-834.

Tischendorf, G., Förster, H.J., Gottesmann, B., 2001. Minor- and trace-element composition of trioctahedral micas: a review. Mineralogical Magazine, 65, 249-276.

Tuttle, O.F., Bowen, N.L., 1958. Origin of granite in the light of experimental studies in the system $NaAlSi_3O_8$-$KAlSi_3O_8$-SiO_2-H_2O. Geological Society of America Memoir, 74, 1-153.

Villaseca, C., Barbero, L., 1994. Chemical variability of Al-Ti-Fe-Mg minerals in peraluminous granitoid rocks from Central

Spain. European Journal of Mineralogy, 6, 691-710.

Villaseca, C., Barbero, L., Rogers, G., 1998. Crustal origin of Hercynian peraluminous granitic batholiths of central Spain: petrological, geochemical and isotopic (Sr, Nd) constraints. Lithos, 43, 55-79.

Villaseca, C., Downes, H., Pin, C., Barbero, L., 1999. Nature and composition of the lower continental crust in central Spain and the granulite-granite linkage: inferences from granulitic xenoliths. Journal of Petrology, 40, 1465-1496.

Villaseca, C., Eugercios, L., Snelling, N., Huertas, M.J., Castellón, T., 1995. Revista de la Sociedad Geológica de España, 8, 129-140.

Villaseca, C., Herreros, V., 2000. A sustained felsic magmatic system: the Hercynian granitic batholith of the Spanish Central System. Transactions of the Royal Society of Edinburgh: Earth Sciences, 91, 207-219.

Villaseca, C., Orejana, D., Paterson, B.A., Billstrom, K., Pérez-Soba, C., 2007. Metaluminous pyroxene-bearing granulite xenoliths from the lower continental crust in central Spain: their role in the genesis of Hercynian I-type granites. European Journal of Mineralogy, 19, 463-477.

Villaseca, C., Pérez-Soba, C., 1989. Fenómenos de alcalinización en granitoides Hercínicos de la Sierra de Guadarrama (Sistema Central). Cuadernos do Laboratorio Xeolóxico de Laxe, 14, 201-212.

Webster, J.D., Rebbert, C.R., 1998. Experimental investigation of H_2O and Cl solubilities in F-enriched silicate liquids: implications for volatile saturation of topaz rhyolite magmas. Contributions to Mineralogy and Petrology, 132, 198-207.

Whalen, J.B., 1983. The Ackley City Batholith, southeastern Newfoundland: evidence for crystal versus liquid-state fractionation. Geochimica et Cosmochimica Acta, 47, 1443-1457.

Whalen, J.B., Currie, K.L., Chappell, B.E., 1987. A-type granites: geochemical characteristics, discrimination and petrogenesis. Contributions to Mineralogy and Petrology, 95, 407-419.

Xiaolin, X., Zhenhua, Z., Jinchu, Z., Bing, R, Mingyuan, L., 1998. Partitioning of F between aqueous fluids and albite granite melt and its petrogenetic and metallogenetic significance. Chinese Journal of Geochemistry, 17, 303-310.

Zaraysky, G.P., Alfereva, J.O., Udoratina, O.V., 2007. Geochemical features of the Etyka tantalum deposit in Eastern Transbaikalia. Stellenbosch University (South Africa), Sixth International Hutton Symposium, 232-233.